



Contents lists available at ScienceDirect

Journal of King Saud University – Science

journal homepage: www.sciencedirect.com

Investigation of erosion-corrosion of aluminium alloy composites: Influence of slurry composition and speed in a different mediums

Pradeep Kumar Yadav, Gajendra Dixit*

Department of Mechanical Engineering, Maulana Azad National Institute of Technology, Bhopal 462003, India

ARTICLE INFO

Article history:

Received 13 December 2017

Accepted 3 February 2019

Available online 6 February 2019

Keywords:

SiC/TiB₂ composite

FESEM

EDS

Marine media

Slurry

Interface

Microstructure

ABSTRACT

In the present study, an effort has been taken to fabricate and compare the erosion-corrosion of aluminium alloy (ADC12) based composite as ADC12-7%SiC and ADC12-7%TiB₂ in Basic, Acidic, Seawater and Aqueous atmosphere. TiB₂ reinforced composite revealed better hardness when compared to that of SiC composite. Erosion-corrosion of aluminium alloy composites were performed at different erodent concentrations (40, 60, 80 wt%) and a speed of 1000, 1500 revolution per minute. It is marked by the study that composites show ameliorate wear resistance than alloy at all speeds and all concentrations except in Basic medium. Microstructural analysis elicited Al-Si interfaces to be a preferential site for corrosion attack. Addition of reinforcement reduces the metallic area for erodent attack; hence composites show less material loss than the alloy. Among composites, TiB₂ reinforcement composite show ameliorates wear resistance irrespective of speed, slurry concentration, and slurry medium. However, regardless of the material, the material loss at 1000 rpm is more than 1500 rpm in Basic media. Based on the analysis, Material removal has the following order in different mediums as; Basic > Acidic > Marine > Water. © 2019 The Authors. Production and hosting by Elsevier B.V. on behalf of King Saud University. This is an open access article under the CC BY-NC-ND license (<http://creativecommons.org/licenses/by-nc-nd/4.0/>).

1. Introduction

Discontinuously reinforced aluminium matrix composites (DRA) are widely used for transporting medium for sand, gravel, coal, limestone and various metal ores but, due to suspended particles in material causes erosion-corrosion in pipeline components such as constrictions, automobile industry, valves, bends and tee junctions (Rawal, 2001; Miracle et al., 2001; Thomas and King, 1993; Hunt and Miracle, 2000; Nicholas, 1995; Bharath et al., 2014; Kumar et al., 2015). Compared with common ceramics TiB₂ particles possess greater Mechanical and Thermal properties (Gao et al., 2015). Material losses by corrosion effect aggravated by erosive/abrasive action and create a massive problem in industrial applications such as turbines, agriculture equipment, pumps put

Abbreviations: Wt, Weight; rpm, Revolution per minute; EDS, Energy dispersive spectrometer; pct, Percentage.

* Corresponding author.

E-mail addresses: pradeepyadav793@gmail.com (P.K. Yadav), dixitgajendra1@gmail.com (G. Dixit).

Peer review under responsibility of King Saud University.



<https://doi.org/10.1016/j.jksus.2019.02.003>

1018-3647/© 2019 The Authors. Production and hosting by Elsevier B.V. on behalf of King Saud University.

This is an open access article under the CC BY-NC-ND license (<http://creativecommons.org/licenses/by-nc-nd/4.0/>).

differentially. Study of erosion-corrosion of Al alloy composites demanded by the situation where mechanical and corrosive wear are in action. Most of the studies on Al alloy composites are carried out to evaluate the physical and Tribological properties. Some experiment has been done to assess the individual effect of erosion-corrosion in the different mediums (Hihara and Latanision, 1994; Feng et al., 1998; Deuis et al., 1996).

Nguyen et al. (2014) have studied erosion rates on stainless steel for different testing time and impact velocity. In their work, erosion rate decreased with time and increased with increase in velocity. Nguyen et al. (2016) reported the transition on erosion profile from “W” shape to a “U” shape. Kumar et al. (2016) revealed that Al alloy with TiB₂ shows better corrosion resistance. It is acknowledged that DRAs have better abrasive/sliding wear properties as compared to the alloy. Being used in corrosive mediums DRAs composites exhibits lower corrosion resistance than matrix alloy (Deuis et al., 1996). The causes of material loss in the corrosive environment include erosion wear, corrosive wear, and abrasive wear by the preferential attack at reinforcement /matrix interfaces, micro cutting, micro-grooving, breaking and partial remotion of ceramic particle (Modi et al., 1999; Saxena et al., 1993; Modi et al., 1992).

Further, the erosion immunity of composite increased by increasing reinforcement weight percentage, and after a certain fraction of reinforcement, composites show a little additional rise in wear resistance with the enhanced tendency of fracture and

remotion of reinforcement (Turenne et al., 1990). Ceramics such as SiC, Al₂O₃, TiC, B₄C, and TiB₂, etc., are being used as reinforcements. Among all reinforcements, SiC is chemically favorable and forms an adequate bond with the metal matrix without forming inter-metallic phase. SiC has another benefit as good thermal conductivity, hardness, mechanical properties, machinability and wear resistance (Khan and Dixit, 2018; Dixit and Khan, 2014; Khan and Dixit, 2017). Furthermore, TiB₂ owing to good fracture toughness, high “melting point, hardness, elastic modulus and good thermal” stability (Basu et al., 2006) has made it a potential reinforcement in Al matrix alloys. TiB₂ ceramic particles do not respond with liquefied aluminium and hence avoid the formation of brittle products on the particle-matrix interface. TiB₂ particles reinforced aluminium reveals better wear resistance (Smith and Chung, 1996; Christy et al., 2010). With compliments to chemical constancy, TiB₂ is more immune for oxidation in the atmosphere for 1100 °C; currently, TiB₂ appears to be fixed to practical applications in areas as impact resistant agricultural units, armor, tools, furnace crucibles, nuclear reactor and wear resistant coatings. It is used as inoculants in aluminium for refining grain size. TiB₂ coating may be used to furnish wear and corrosive resistance to a robust substrate. Material removal in erosion-corrosion causes pitting and fracture, fragmentation and partial removal of the dispersoid. Most of the study reported corrosion attack took place preferentially aluminium/reinforcement interfaces. However, a few investigators have reported that pit formations in composites are frequent in the composite as compare to matrix alloy. A few investigators also reported that inclusion of reinforcement in matrix alloy restricted the growth of pits (Trzaskoma, 1990; Muller and Galvele, 1977). Thus, in the present study, we can compare the material removal of a SiC and TiB₂ reinforced Al alloy composite in Basic, Acidic, Seawater/marine/saltic and an aqueous medium. The outcome of suspended erodent concentration, rotational speed and study of the worn surface by SEM has also been investigated to explain the wear mechanism.

2. Experimental

2.1. Material

The present study uses an Al-Si alloy (ADC-12) and its composites ADC12-7%SiC, ADC12-7%TiB₂ with SiC and TiB₂ reinforcement. The chemical compositions of ADC12 alloy are shown in Table 1. SiC and TiB₂ Particles for reinforcement taken as the particle size of 5 to 40 μm.

Herein, SiC and TiB₂ particles preheated at 1000 °C for 3 h to raise the bonding by eliminating the absorbed hydroxides, moisture, and gases. The temperature of the furnace was raised to 750 °C to melt base alloy entirely and then the preheated reinforcements were added. 2 g of magnesium is added to raise the bonding of reinforced particles. Mechanical stirring is done for 20 min at an average speed of 350 rpm. The liquefied materials were then poured into the sand mold by gravity casting. The dimensions of the mold are 150x80x10 mm in plate shape for sample fabrication.

2.2. Microstructure and EDS

For microstructure analysis, samples were mechanically polished using standard metallographic technique and etched with Keller's reagent and observed in HR FESEM (Zeiss, ULTRA Plus).

2.3. Erosion-corrosion tests

The erosion-corrosion test was carried out in slurry erosion tester TR-40 (Model-Ducom Bangalore India). For testing purpose, the

Table 1

Chemical compositions of aluminium alloys ADC (in wt.%).

Element	Si	Mn	Mg	Cu	Fe	Ni	Al
ADC-12	10.29	0.12	0.47	1.98	0.75	0.80	Rest

rectangular bar of size 25.4 × 76.2 × 6.35 mm was taken with a hole at the center of size 8.5 mm for holding a sample in the slot. The experiments were conducted for 60 min.

The erosion-corrosion test was carried out in Basic (3.5% sodium hydroxide, pH 11.5), acidic environment (1000 ml water +0.5 ml hydrogen chloride +0.4 ml sulfuric acid solution at pH of 2.5) simulating synthetic mine water atmosphere, marine environment (3.5% NaCl, pH 7.5) and an aqueous medium. Sand sizes of 700–900 μm were used in the solutions. The composition of the sand was further varied as 40, 60, 80 wt% in 600 ml of water. To see the effect of rotational speed the erosion-corrosion test was conducted at two different speeds 1000, 1500 rpm respectively. The worn-out surfaces and the compositional analysis have further been carried out using electron microscopy.

2.4. Hardness

The hardness of Al alloy and SiC/TiB₂reinforced composites in as-cast conditions were measured using Vickers hardness (Hv) testing machine (model: VM 50, FIE). The specimen was polished metallographically, and the opposite sides of the samples were made perfectly parallel before hardness measurement. The Vickers

Table 2

Hardness values of ADC12 and composites.

S. No	Material	Vickers hardness
1	ADC12	90
2	ADC12-7%SiC	98
3	ADC12-7%TiB ₂	105



Fig. 1. Specimen for slurry erosion tester.

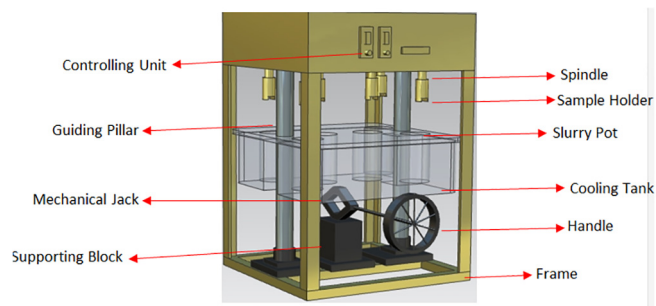


Fig. 1a. Model of slurry erosion tester (TR-40) [Khan, M. M., & Dixit, G. (2017)].

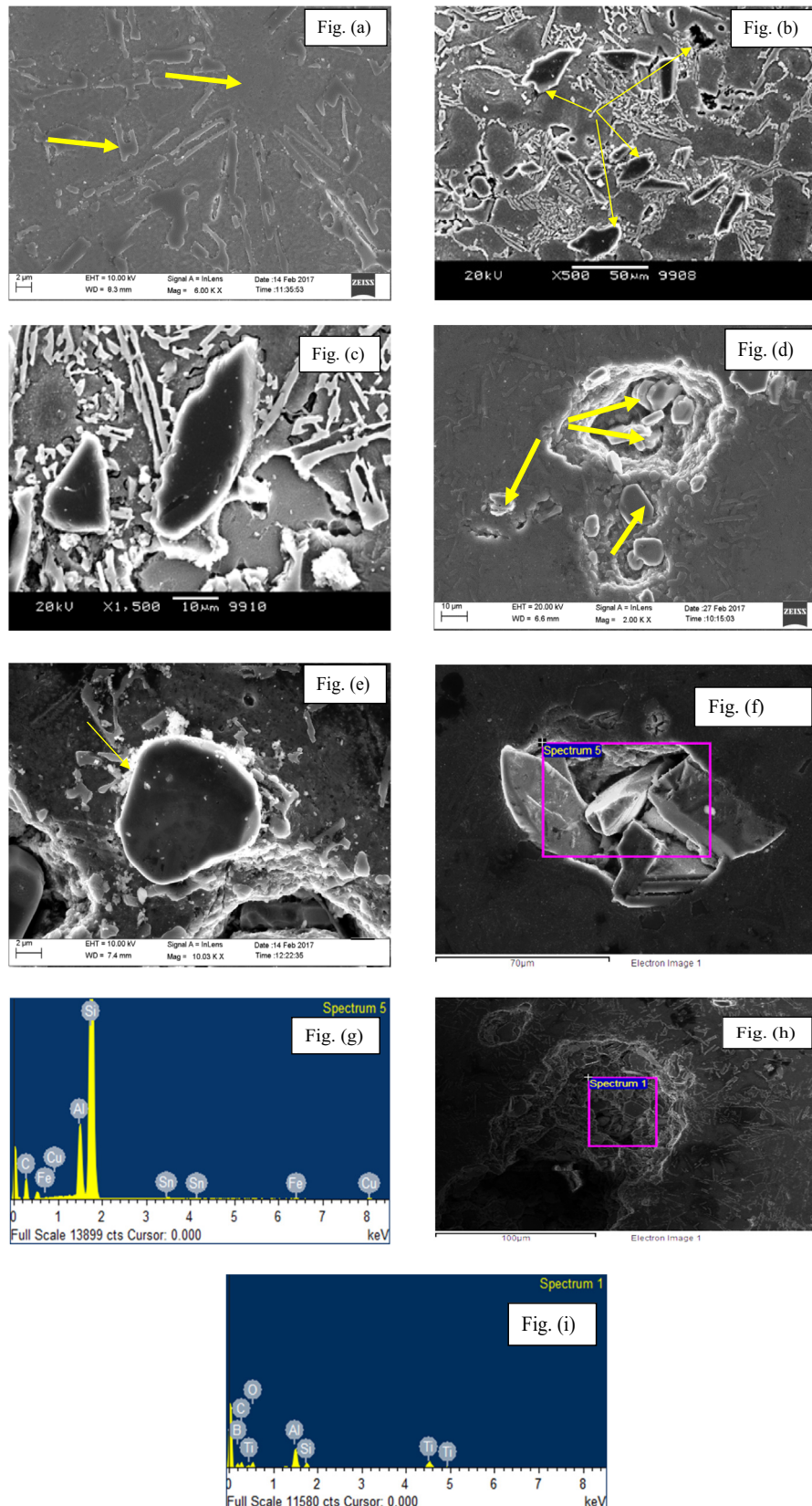


Fig. 2. . The microstructure of ADC12 and composites (a) A scanning electron micrograph of as-cast ADC12 alloy showing aluminum dendrites and eutectic silicon solidifying in the inter-dendritic region and around dendrites. (b) A Micrograph of as-cast ADC12-7% SiC composite showing secondary aluminum dendrites eutectic silicon in the dendritic spacing and around the dendrites and SiC particles distributed in the matrix. (c) A magnified image of as-cast ADC12-7% SiC composite showing entrapment of SiC particle in the last freezing eutectic liquid (d) A distribution of TiB₂ ceramics in the ADC-12 alloy. (e) A magnified image of as-cast ADC12-7% TiB₂ composite showing entrapment of TiB₂ particle in the last freezing eutectic liquid. (g) Confirms silicon carbide particle in (f) for spectrum 5. The microstructure of (h) depicts the presence of titanium diboride particles in (i) for spectrum 1.

hardness of the specimen was obtained at an applied load of 5 kgf with a dwell time of 5 s using diamond pyramid indenter. Five indents were taken to report an average value.

3. Result

3.1. Microhardness analysis

Table 2 shows the hardness values of Al alloy and SiC/TiB₂ Composites. Each composite showed a higher value than the base alloy due to the dispersion of fine and reinforcement particles. The TiB₂ reinforced alloys showed higher value (105) when compared to the SiC reinforced alloy (98) is attributed to the high hardness of TiB₂ particles.

Further, the reduction in hardness reveals the decrease in indentation depth, which could be linked to the dispersion of residual tensile stresses in ceramics. Hardness can also be dropped by microcracking or pores formation (King et al., 2013). That is why the increase was expected in TiB₂ particulate composites (See Figs. 1 and 1a).

3.2. Microstructure analysis and EDS

The microstructure of the Al-Si alloy (ADC12) and composites (ADC12-7%SiC, ADC12-7%TiB₂) was observed in the SEM and shown in Fig. 2. Fig. 2(a) micrograph of as-cast ADC12 alloy elicits aluminium dendrites and silicon solidifying in the inter-dendritic region around dendrites. Fig. 2(b) reveals the homogeneous distribution of SiC ceramic particles as reinforcement in Al alloy. Fig. 2(c) shows the higher magnification micrograph of as-cast ADC12 with ADC12-7% SiC composite showing entrapment of SiC ceramics particle in the last freezing eutectic liquid. Fig. 2(d) show the micrograph of as-cast ADC12-7%TiB₂ composite in which secondary aluminium dendrites eutectic silicon in the dendritic spacing and around dendrites and TiB₂ particles in the matrix were witnessed.

A higher magnification micrograph of as-cast ADC12-7% TiB₂ composite showing entrapment of TiB₂ particle in the last freezing eutectic liquid is shown in Fig. 2(e). The interface boundary between the reinforced particle and aluminium silicon matrix is also seen.

3.3. Morphology and EDS of reinforced particles

Fig. 3(a) and (c) show the morphology of silicon carbide and titanium diboride respectively. It can be seen in the figure that the shape of SiC particle is irregular with edges and shape of TiB₂ is hexagonal. Fig. 3(b) and (d) Reveals EDS for spectrum 1 and spectrum 3 respectively which confirms the presence of silicon carbide and titanium diboride particles.

3.4. Erosion-corrosion behavior

Effect of varying sand concentration and speed on the erosion-corrosion of aluminum alloy and ADC12-7%SiC, ADC12-7%TiB₂ composites in Basic medium (Fig. 4(a), (b)), acidic medium (Fig. 4(c), (d)), marine medium (Fig. 4(e), (f)), aqueous medium (Fig. 4(g), (h)) is shown in Fig. 4. Fig. 4(a) and (b), show graph between weight loss versus slurry composition for ADC12, ADC12-7%SiC, ADC12-7%TiB₂ in the basic medium as the variation of slurry concentration and at a speed of 1000 rpm, 1500 rpm respectively. Alloy show least material removal as compared to composites, and at 1500 rpm material removal exhibits less than at 1000 rpm. Among composites, TiB₂ composite showed less material loss than the SiC composite is attributed to the higher hardness of TiB₂ reinforced alloys. Weight loss increases with increase in the slurry concentration irrespective of material. Also, the basic medium showed maximum material removal as compared to other mediums. Fig. 4(c), (d), show graph between weight loss versus slurry composition for alloy and composites in acidic media. Plots depict that as the concentration of suspended erodent particles

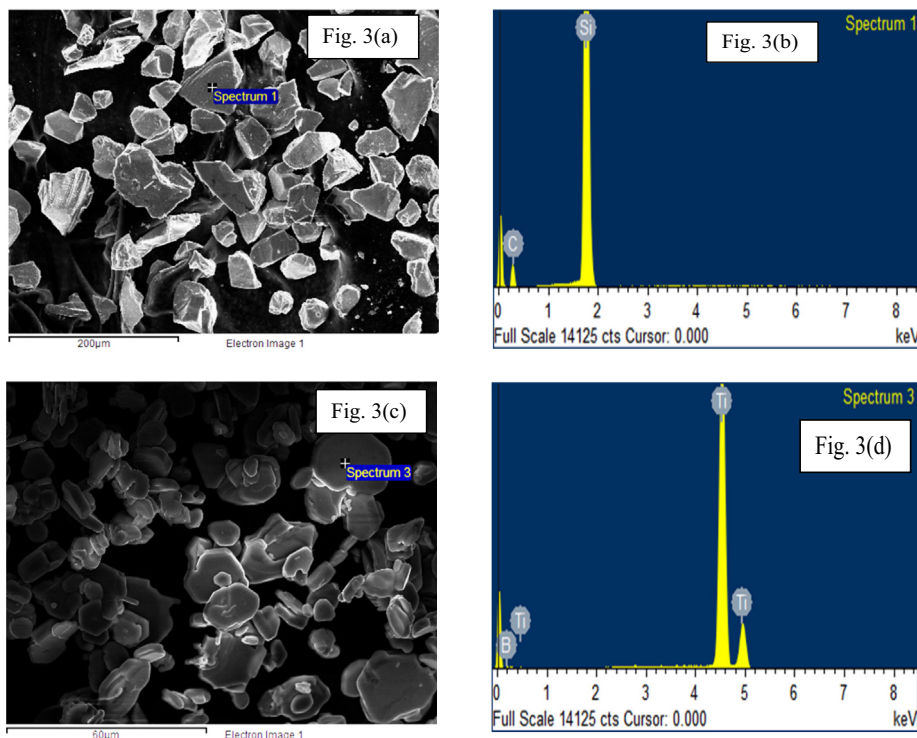


Fig. 3. (a) and (c) shows the morphology of silicon carbide and titanium diboride respectively. (b) and (d) reveals EDS for spectrum 1 and spectrum 3 respectively.

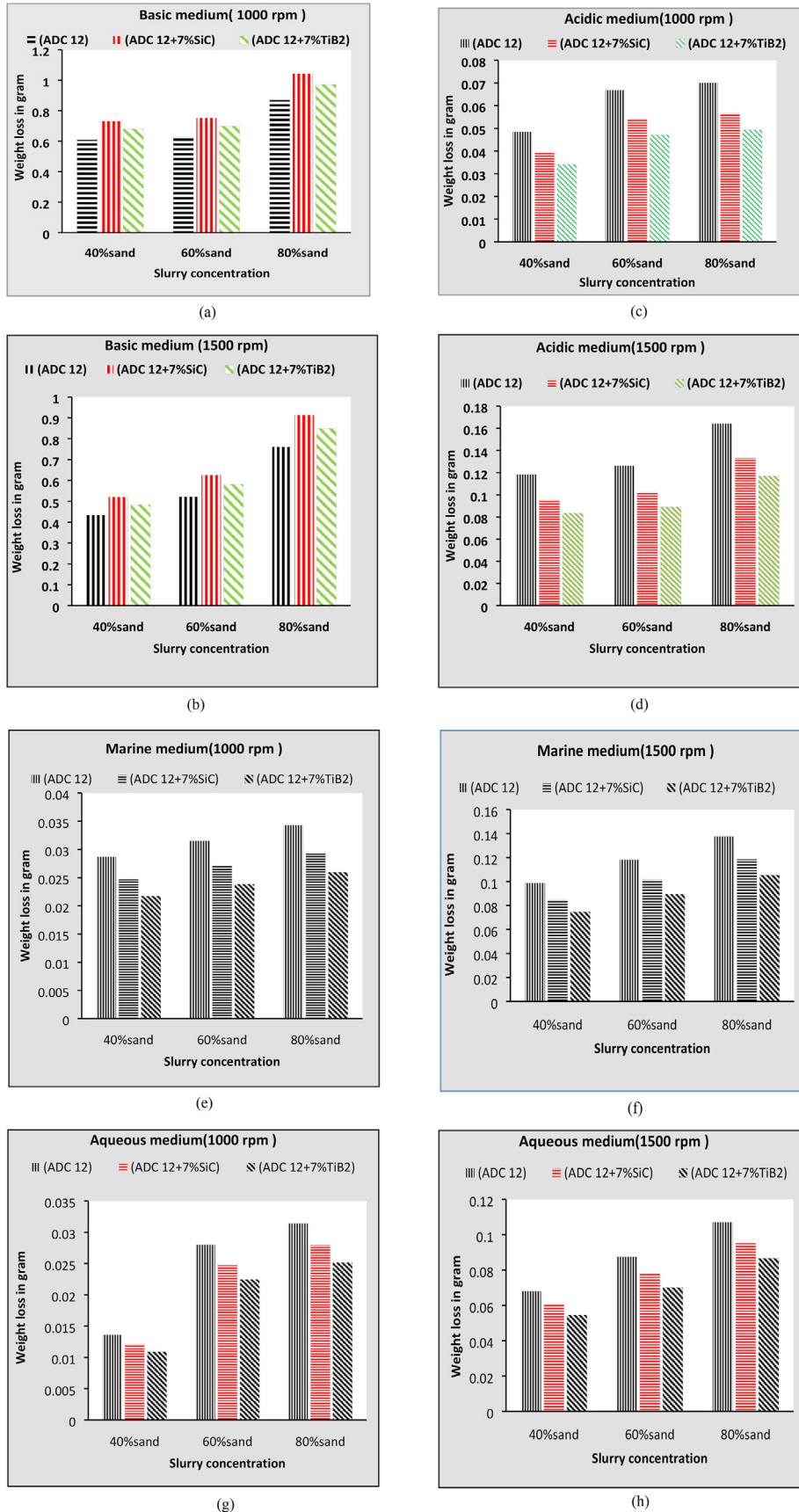


Fig. 4. (a-h) Graph between Weight loss versus slurry concentration in the different slurry mediums. (i-j) Graph between Weight loss versus variation in slurry mediums for 80% sand concentration and 1000 rpm. (k-l) Graph between Weight loss versus variation in slurry mediums for 80% sand concentration and 1500 rpm.

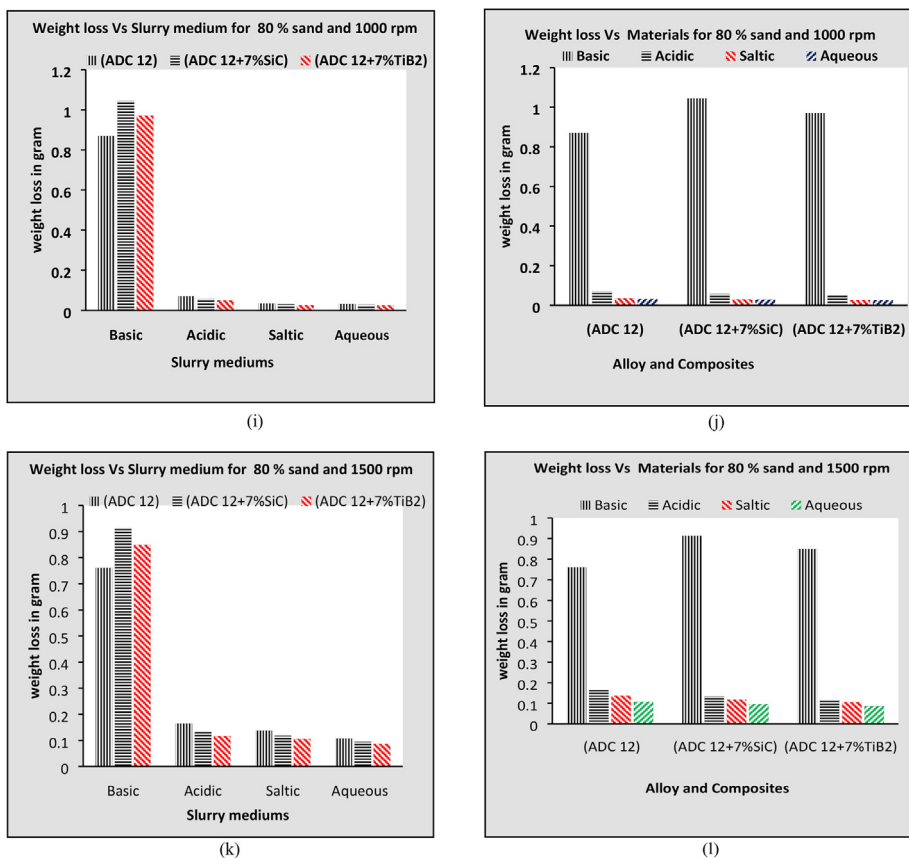


Fig. 4 (continued)

increases then material removal increases irrespective of material, but in acidic medium material, removal is less than that of basic media. Composites show less material loss than the alloy at all slurry concentration and speeds. Among composites, TiB₂ ceramic composite show better wear resistance than the SiC composites is due to the high hardness of TiB₂ based composites. This phenomenon is also seen in the case of the marine and aqueous medium. Effect of varying 80% sand concentration and 1000 rpm speed on the erosion-corrosion of aluminum alloy and ADC12-7%SiC, ADC12-7%TiB₂ composites in different mediums are shown in Fig. 4(i), (j). Fig. 4(i), reveals that for all materials weight loss is maximum in Basic media and minimum in aqueous media and in basic media alloy show better wear resistance than the composites. In other media, composites show better wear resistance than the alloy. Among composites, titanium diboride reinforced composites show better wear resistance. Fig. 4(j) show graph between weight loss versus material composition as ADC12, ADC12-7%SiC, ADC12-7%TiB₂ in the different mediums. Graph between these parameters clearly depicts that all material has maximum weight loss in basic media and minimum in aqueous media. Beside this ADC12-7%SiC composite have maximum weight loss in basic media as compared to ADC12, ADC12-7%TiB₂. Effect of varying 80% sand concentration and 1500 rpm speed on the erosion-corrosion of aluminum alloy and ADC12-7% SiC, ADC12-7%TiB₂ composites in different mediums are shown in Fig. 4(k), (l). Fig. 4(k), reveals that for all materials weight loss is maximum in Basic media and minimum in aqueous media and in basic media ADC12 have less material loss, and among composites, ADC12-7%TiB₂ have more wear resistance than ADC12-7%SiC composite. Fig. 4(j) show graph between weight loss versus material composition as ADC12, ADC12-7%SiC, ADC12-7%TiB₂ in the different mediums. Graph between these material

variation clearly depicts that all material has maximum weight loss in basic media and minimum in aqueous media. Beside this ADC12-7%SiC and ADC12-7%TiB₂ composite have maximum weight loss in basic media as compared to ADC12. All material has more weight loss in the acidic medium as compared to salty medium.

3.5. Eroded-corroded surface

The erosion-corrosion of Al alloy composites were investigated by SEM with the aim of understanding the mechanism of weight loss as a function of experimental parameters. Fig. 5(a) depicts the eroded surface of the alloy at 80 wt% sand in the slurry, and 1500 rpm reveals an area of light marks, in addition to grooves are also found. Grooves show resistance to abrasion. Fig. 5(b) reveals pitting surface at 80 wt% of sand suspension in slurry and 1000 speed of rotation. The corrosion product removed by the action of the slurry at high speed and high composition hence clear surface come across by pits and grooves which can be made because of resistance to abrasion. It is also shown that corrosive attack prefers at Al/Si interfaces. The SiC ceramic particle in alloy does change site of preferential attack but reduces the net surface area for erosion-corrosion due to an intrusion of reinforced particles. That is the reason composites depicts less material removal than alloy, In Fig. 5(c) grooves, are found. However, there is no disengagement of SiC ceramic particles found in the composite. There is no sign of interface de-cohesion. In Fig. 5(d) show the eroded corroded surface at 1500 rpm and 80% of sand suspension in the slurry. In this case, the impairment to the SiC ceramics particle is severe, and the particle breaks into smaller pieces. It is revealed from the eroded surface that SiC ceramic was not pullout

from the aluminium matrix because of erosive/abrasive action and no sign of interface debonding was seen. Fragmentation of SiC occurs at high speed because of low toughness showed by silicon carbide particles (Patel, 2018a,b). The TiB_2 particle in alloy does not change the site of preferential attack but reduces the net surface area for erosion-corrosion due to the intrusion of reinforced particles. That is the reason by composite reveals better wear immunity than alloy. Fig. 5(e) depicts the grooves which reveal restriction to abrasion. The thinner groove is formed in the alloy as compared to SiC reinforced composite. Grooves are not continuous here, being TiB_2 particles resist the abrasive action through the interface. Thus, here wear mechanism is the sum of micro cutting, ploughing and surface abrasion. Fig. 5(f) depicts the agglomeration of TiB_2 particles in composites and formation of light of wear marks at 80 wt% sand and 1500 rpm speed. It could be concluded here that no evidence of particles pulls out and fracture of reinforced particles. In Fig. 5(g)–(i) show the FESEM of eroded-corroded worn surface revealed that ADC12 alloy received high corrosive assault in basic media and the surface of alloy became

porous. In the case of composites, because of corrosion, surface leads dissipation of primary phase aluminium dendrites leaving behind the silicon network. Subsequently, erosion extends, and silicon comes out in the form of a needle. This leads to voids constitution around reinforced particles. Thus, reinforced particles easily pullout from the material by abrasive and erosive action. This is the reason behind more remotion of material in composites than alloy (Patel, 2018a,b). Additionally, the material removal properties were improved on increasing speed, the abrasive capacity of slurry decreases leads to less loss of material because in basic media material is removed by corrosion. Interface bonding between titanium boride particles and alloy are better than silicon carbide due to which former revealed better wear immunity. In Fig. 5(j)–(l) show eroded-corroded worn surface of ADC12 alloy which received high corrosive assault in acidic medium but not much as in basic medium consequently worn surface became porous due to pitting action. For acidic medium erosion is the prevailing mode of weight loss. whenever alloy is exposed to acidic media, they form hydroxides. However, the addition of erodent particles

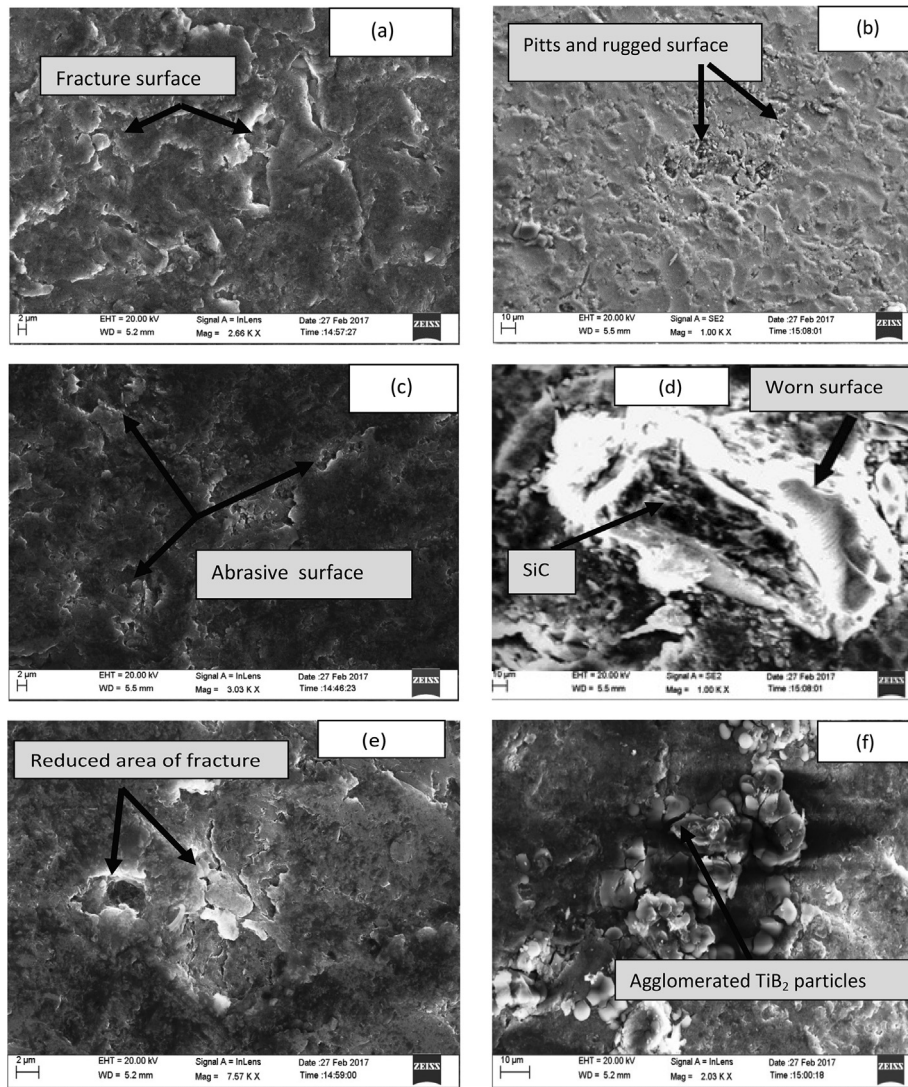


Fig. 5(a–f). . The eroded-corroded surface of ADC12 and ADC12-7%SiC, ADC12-7% TiB_2 composites in marine solution at a different speed and different slurry concentration. (a) Erosion-corrosion of ADC12 at 80 wt pct sand composition and 1500 rpm depicts more fracture surface. (b) Erosion-corrosion of ADC12 at 80 wt pct and 1000 rpm reveals material loss due to pitting action. (c) Resistance to abrasion surface for the ADC12-7%SiC composite at 80 wt pct sand composition and 1000 rpm. (d) The broken particle of SiC shown in SiC reinforced site at 80 wt pct sand in the slurry, and 1500 rpm speed (e) Erosion-corrosion of ADC12-7% TiB_2 at 80 wt pct sand and 1500 rpm speed shows fracture on the surface due to the abrasive action of sand in the slurry. (f) Erosion-corrosion of ADC12-7% TiB_2 at 80 wt pct sand and 1500 rpm speed depicts agglomeration of ceramic particle and grooves.

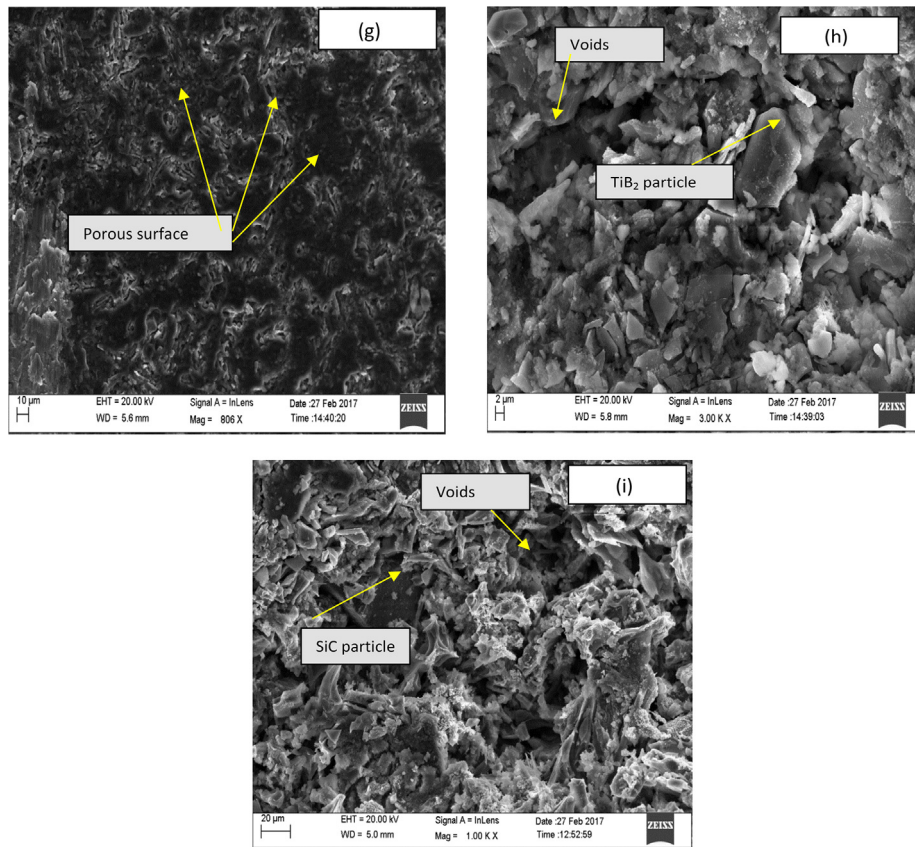


Fig. 5(g-i) . The eroded-corroded surface of ADC12 and ADC12-7%SiC, ADC12-7%TiB₂ composite in basic media. (g) The microstructure of eroded-corroded surface of ADC12 alloy depicting porous surface due to corrosive attack. (h) The eroded-corroded surface of ADC12-7 pct TiB₂ composite is depicting the voids formed around the TiB₂ Particle due to the fall of silicon. (i) The eroded-corroded surface of ADC12-7 pct SiC composite depicting the voids formed around the SiC particle due to the fall of silicon.

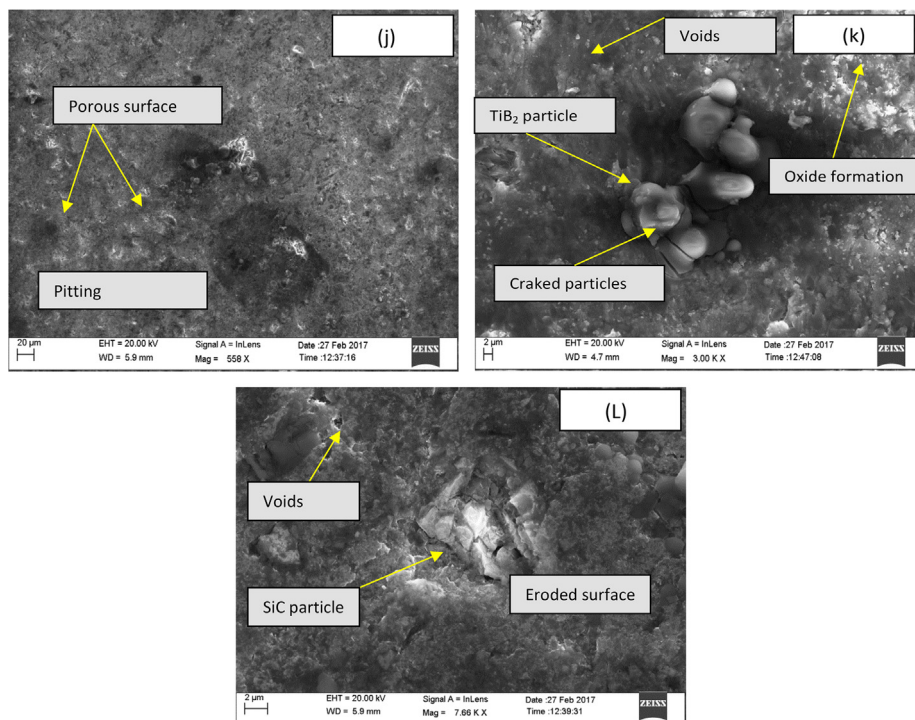


Fig. 5. (j-l) . The eroded-corroded surface of ADC12 and ADC12-7%SiC, ADC12-7%TiB₂ composite in acidic media. (j) The microstructure of eroded-corroded of ADC12 alloys depicting porous surface due to corrosive attack. (k) The eroded-corroded porous surface of ADC12-7%TiB₂ composite depicting the voids formed and agglomeration of TiB₂ particle and Cracked particles due to abrasive action at 80 pct of sand concentration and 1500 rpm. The formation of oxide layer on the surface of the composite. Voids are created elsewhere due to pitting action. (l) The eroded-corroded porous surface of ADC12- 7%SiC reinforced composite depicting the voids formed around the SiC particle due to the fall of silicon.

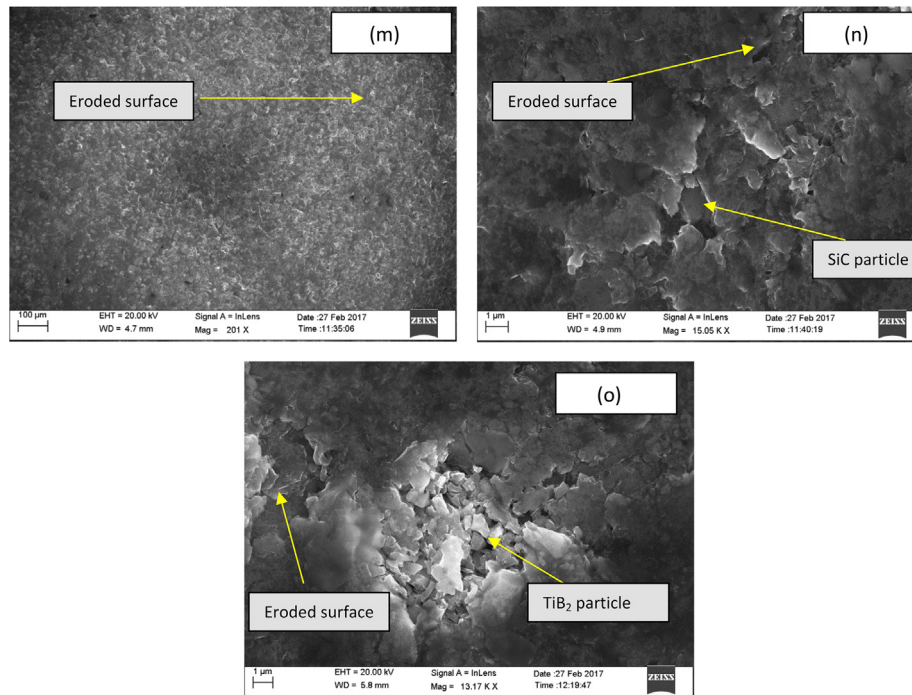


Fig. 5(m–o). Shows worn surfaces of alloy, its silicon carbide and titanium diboride composite respectively in an aqueous slurry at 80% sand concentration and 1500 rpm.

in slurry continuously abrades the passive layer leading to the vulnerability of the fresh layer. Thus, the alloy is more prostrate to corrosion attack. In case of composites, corrosive attack leads to dissipating of primary phase aluminium dendrites leaving behind the silicon plate shape network. The worn surface of alloys and SiC/TiB₂ reinforced composites are respectively shown in Fig. 5 (m)–(o). The worn surface reveals less roughness than the other media. In this mild groove are seen indicating surface subjected to plastic deformation, voids, micro cuts, and pits due to scratching of high energy erodent. Presence of ceramic particles further reduces net area hence less surface to be attacked by suspended particles.

4. Discussion

4.1. Effect of reinforcement on the erosion-corrosion behavior

The pH value of the marine solution is 7.5. It is well known from the pH-potential-pourbaix diagram for Al that Al passivity in the pH value of 4–8 by the rapid formation of the Al₂O₃ passive film in marine (sea water) (Davis, 1993). Previous investigations reveal the establishment of a stable Al₂O₃ passive film in marine solution (Saraswathi et al., 2001). Whenever there is an erodent's available in the slurry, then erodent continuously scratches the passive layer heading to the vulnerability of fresh surfaces. Material removal process comprises preferential sites in Al-Si interfaces or case of foreign particles interface between primary phase Al alloy or silicon dendrites with reinforced particles also subjected to preferential attack. Addition of ceramic particles (SiC, TiB₂) doesn't change the preferential sites for corrosive assault, and an attack occurs at the Al-Si interface. SiC, TiB₂ ceramic particle is an insulator in nature and does not susceptible to corrosion attack but SiC is coherent with the intermediate products such as Al₄C₃, or some preferential precipitation of intermetallic takes place (Wu and Lavernia, 1991). A TiB₂ particle composite show some susceptibility to acidic medium. Whereas, the ADC12 alloy having an improved wear property in the present SiC composite, no chance of constitution of Al₄C₃ at

the low temperature of castings and ADC12 consists of the more considerable amount of silicon (11.5 wt%) which inherits formation of Al₄C₃. The presence of ceramic (SiC and TiB₂) particles disrupted the continuity of the passive layer in the composites. The inclusion of ceramic particles as reinforcement reduces the effective metallic area exposed to corrodant in composites hence hinder pits formation. Thus, the inclusion of ceramic particles depicts better wear resistance.

4.2. Effect of varying erodent concentration and speed

Erosion-corrosion in marine media is a typical phenomenon. Generally, erosion-corrosion is a composite process in corrosive media and depends upon corrosive wear (W_c), Erosive wear (W_e) due to the impact of erodent particle suspended in slurry media, abrasive wear (W_a) due to abrading action on the surface of the material. In this experiment, it can be found that aluminium composites exhibit better wear immunity (inverse of weight loss) as compared to alloy irrespective of all slurry concentrations and all speed except in case of basic media. As erosive wear is a function of the energy of eroded particles and severity of the attack, which increases with the energy. The energy of eroded particles directly coupled with the energy of striking particles. Thus, the wt loss of alloy and composites increased as speed increased from 1000 to 1500 rpm but at higher speed say 1500 rpm, the mobility of erodent particles decreased because now erodent has less time to make an effective impact and scratch over the material. Further intercollision rebounds increase at higher speeds and high sand concentrations thus abrasive actions increases at 1500 rpm. TiB₂ composite depicts better wear immunity as compared to SiC composite is attributed to the better fracture toughness than SiC. At extravagantly speed fragmentation depicts in SiC particles Fig. 5 (d) and TiB₂ in Fig. 5(k). The intensity of erosive assault is subjected to erodent particle energy. The more energy of impinging erodent, the more severe will be the attack. Thus, the speed of rotation is increased from 1000 to 1500 rpm then wt loss also increases. Enhancement in the energy of striking particle the greater will be

damage to the SiC, TiB₂ particles. However, SEM observation did not confirm that ceramic reinforcement particle pulls out occurred under these conditions. Thus, the protruding of ceramic reinforced particles reduced the damage to the aluminium matrix and in turn mended the wear immunity at all the speeds. However, at higher speeds, say 1500 rpm, the suspended erodent's particles scratch over the surface instead of making any sensible impact. Further, higher speed, chances of abrasive wear increased due to sliding action. Additionally, chances of scratching on the material, more at high speeds. All these factors cumulatively increased material removal at a speed of 1500 rpm and high sand concentration. Because of low toughness of Silicon carbide particle and greater abrasive wear immunity of TiB₂, the TiB₂ ceramic composite at high speed depicts the less material removal than alloy and silicon carbide composite.

5. Conclusion

The compositional analysis confirms the presence of SiC and TiB₂ ceramic particles. Composites exhibited better wear resistance than the alloy, and among composites, TiB₂ based composite show better wear immunity at all speed and slurry concentration. The weight loss enhanced with an increase in the composition of sand in Acidic, Marine and Aqueous medium irrespective of material. In Basic media, composites show more material removal than the alloy and among composite TiB₂ exhibits better wear resistance. Erosion-corrosion found prevalent mode in material removal at 1000 rpm, and 1500 rpm abrasion-corrosion was found to be prevalent in material removal. Corrosion is the prevalent mode of mass removal in Basic media. Material removal decreases in the different erosive-corrosive medium as; Basic > Acidic > Saltic > Aqueous. Material removal occurs because of erosion, abrasion, and corrosion which alters the site of material by plastic deformation, voids formation and repeated attack of erodent's particles on the material surface.

References

- Rawal, S.P., 2001. Metal-matrix composites for space applications. *Jom* 53 (4), 14–17.
- Miracle, D.B., Donaldson, S.L., Henry, S.D., Moosbrugger, C., Anton, G.J., Sanders, B.R., Hrivnak, N., Terman, C., Kinson, J., Muldoon, K., Scott Jr, W.W., 2001. *ASM Handbook*. ASM International, USA, pp. 107–119.
- Thomas, M.P., King, J.E., 1993. Effect of thermal and mechanical processing on tensile properties of powder formed 2124 aluminium and 2124 Al-SiC p metal matrix composite. *Mater. Sci. Technol.* 9 (9), 742–753.
- Hunt, W.H., Miracle, D.B., 2000. Automotive applications of metal matrix composites. *ASM Handbook Compos.* 21, 1029–1032.
- Nicholas, T., 1995. An approach to fatigue life modeling in titanium-matrix composites. *Mater. Sci. Eng. A* 200 (1–2), 29–37.
- Bharath, V., Nagaral, M., Auradi, V., Kori, S.A., 2014. Preparation of 6061Al-Al₂O₃ MMC's by stir casting and evaluation of mechanical and wear properties. *Proc. Mater. Sci.* 6, 1658–1667.
- Kumar, G.P., Keshavamurthy, R., Ramesh, C.S., Bharathesh, T.P., 2015. Mechanical properties of Hot forged Al6061-TiB₂ in-situ metal matrix composites. *Mater. Today: Proc.* 2 (4–5), 3107–3115.
- Gao, Q., Wu, S., Lü, S., Duan, X., Zhong, Z., 2015. Preparation of in-situ TiB₂ and Mg₂Si hybrid particulates reinforced Al-matrix composites. *J. Alloy. Compd.* 651, 521–527.
- Hihara, L.H., Latanision, R.M., 1994. Corrosion of metal matrix composites. *Int. Mater. Rev.* 39 (6), 245–264.
- Feng, Z., Lin, C., Lin, J., Luo, J., 1998. Pitting behavior of SiCp/2024 Al metal matrix composites. *J. Mater. Sci.* 33 (23), 5637–5642.
- Deuis, R.L., Subramanian, C., Yellup, J.M., 1996. Abrasive wear of aluminium composites – a review. *Wear* 201 (1–2), 132–144.
- Nguyen, Q.B., Lim, C.Y.H., Nguyen, V.B., Wan, Y.M., Nai, B., Zhang, Y.W., Gupta, M., 2014. Slurry erosion characteristics and erosion mechanisms of stainless steel. *Tribol. Int.* 79, 1–7.
- Nguyen, V.B., Nguyen, Q.B., Zhang, Y.W., Lim, C.Y.H., Khoo, B.C., 2016. Effect of particle size on erosion characteristics. *Wear* 348, 126–137.
- Kumar, G.P., Keshavamurthy, R., Kumari, P., Dubey, C., 2016. Corrosion behaviour of TiB₂ reinforced aluminium based in situ metal matrix composites. *Perspect. Sci.* 8, 172–175.
- Modi, O.P., Prasad, B.K., Dasgupta, R., Jha, A.K., Mondal, D.P., 1999. Erosion-corrosion characteristics of squeeze-cast aluminium alloy/SiC composites in water and sodium chloride solutions containing sand. *Mater. Sci. Technol.* 15 (8), 933–938.
- Saxena, M., Modi, O.P., Prasad, B.K., Jha, A.K., 1993. Erosion and corrosion characteristics of an aluminium alloy-aluminaFiber composite. *Wear* 169 (1), 119–124.
- Modi, O.P., Prasad, B.K., Yegneswaran, A.H., Vaidya, M.L., 1992. Dry sliding wear behaviour of squeeze-cast aluminium alloy-silicon carbide composites. *Mater. Sci. Eng. A* 151 (2), 235–245.
- Turenne, S., Chatigny, Y., Simard, D., Caron, S., Masounave, J., 1990. The effect of abrasive particle size on the slurry Erosion resistance of particulate-reinforced aluminium alloy. *Wear* 141 (1), 147–158.
- Khan, M.M., Dixit, G., 2018. Abrasive wear characteristics of silicon carbide particle reinforced zinc based composite. *Silicon* 10 (4), 1315–1327.
- Dixit, G., Khan, M.M., 2014. Sliding wear response of an aluminium metal matrix composite: effect of solid lubricant particle size. *Jordan J. Mech. Indus. Eng.* 8 (6).
- Khan, M.M., Dixit, G., 2017a. Effects of test parameters and SiCp reinforcement on the slurry erosive wear response of Al-Si Alloy. *Mater. Today: Proc.* 4 (2), 3141–3149.
- Khan, M.M., Dixit, G., 2017b. Erosive wear response of SiCp reinforced aluminium based metal matrix composite: effects of test environments. *J. Mech. Eng. Sci.* 14, 2401–2414.
- Basu, B., Raju, G.B., Suri, A.K., 2006. Processing and properties of monolithic TiB₂ based materials. *Int. Mater. Rev.* 51 (6), 352–374.
- Smith, A.V., Chung, D.D.L., 1996. Titanium diboride particle-reinforced aluminium with high wear resistance. *J. Mater. Sci.* 31 (22), 5961–5973.
- Christy, T.V., Murugan, N., Kumar, S., 2010. A comparative study on the microstructures and mechanical properties of Al 6061 alloy and the MMC Al 6061/TiB₂/12p. *J. Miner. Mater. Charact. Eng.* 9 (01), 57.
- Trzaskoma, P.P., 1990. Pit morphology of aluminum alloy and silicon carbide/aluminum alloy metal matrix composites. *Corrosion* 46 (5), 402–409.
- Muller, I.L., Galvele, J.R., 1977. Pitting potential of high purity binary aluminium alloys – I. Al Cu alloys. Pitting and intergranular corrosion. *Corros. Sci.* 17 (3), 179–193.
- Khan, M.M., Dixit, G., 2017c. Comparative study on erosive wear response of SiC reinforced and fly ash reinforced aluminium based metal matrix composite. *Mater. Today: Proc.* 4 (9), 10093–10098.
- King, D.S., Fahrenholtz, W.G., Hilmars, G.E., 2013. Silicon carbide-titanium diboride ceramic composites. *J. Eur. Ceram. Soc.* 33 (15–16), 2943–2951.
- Patel, S.K., 2018a. Microstructural and compressive deformation behaviour of aluminium foam filled sections. *Soft Mater.* <https://doi.org/10.1080/1539445X.2018.1528457>.
- Patel, S.K., 2018b. The slurry abrasion wear behavior and microstructural analysis of A2024-SiC-ZrSiO₄ Metal matrix composite. *Ceram. Int.* 44 (6), 6426–6432.
- Davis, J.R., 1993. *Aluminum and Aluminum Alloys*. ASM International.
- Saraswathi, Y.L., Das, S., Mondal, D.P., 2001. A comparative study of corrosion behavior of Al/SiC composite with cast iron. *Corrosion* 57 (7), 643–653.
- Wu, Y., Lavernia, E.J., 1991. Spray-atomized and deposited 6061 Al/SiC p composites. *Jom* 43 (8), 16–23.